An Improvement of Iris Pattern Identification Using Radon Transform

Pattraporn Ariyapreechakul and **Nongluk Covavisaruch**, Non-members

ABSTRACT

This research proposes an improvement of iris personal identification system using Radon transform which is used to extract feature stored as templates in a database. In our research, the system has been tested to find the best system performance with 3 distance functions: regional correlation, Euclidean distance and absolute distance. The test images are from CASIA iris database. Our experimental results reveal that the improved approach greatly increases the system performance for all distance functions. Among the 3 distance functions, the absolute distance gives the best results which reduce EER from 18% (previous approach) to 3.695%.

Keywords: Iris, Feature extraction, Radon transform.

1. INTRODUCTION

have some security modules to protect imposters from accessing them. Cards and/or passwords are typically used for security purpose. However, cards can be stolen while passwords can be forgotten. Hence, biometric is introduced for use in personal authentication. Biometric refers to personal physiological and behavioral characteristics that can be used to authenticate a persons identity. Fingerprints, faces, retinas, and irises are some examples of the physiological characteristics whereas voice, signatures, and gaits, the behavioral characteristics. This research exploits iris pattern for personal identification to identify a person who is registered to the system.

Iris is the tissue located between sclera and pupil. It consists of many complex structures such as freckles, ridges, furrows, crypts, and coronas, etc. Iris pattern is stable and most likely never changes throughout the persons life [1, 2]. Therefore, it is considered a suitable biometric for use in high security systems.

area of iris personal identification over the recent decades. R.P. Wildes [1] has proposed to use Laplacian pyramid for extracting feature and match the templates by normalize correlation combined with Fishers linear discriminant. J. G. Daugmans iris recognition system [3], which is perhaps the most referred-to system, uses Quadrature 2D Gabor wavelet to create a 2,048-bit iris pattern. The error rate is about 0.000083%. R. Sanchez- Reillo et al. [4] have proposed an iris recognition system with a small template size. The iris images for feature extraction are chosen from those between -45 and 45 degrees, and between 135 and 225 degrees. Gabor filter is used to extract feature. The error rate is 3.6 % for 1,860 bits. L. Ma et al. [5] have proposed a new algorithm to represent the iris texture with spatial filter adapted from Gabor filter. C. Chun et al. [6] have introduced an iris recognition system for palm-top application by using Radon transform which reduces computational time by 6 times compared with wavelet transform. B. R. Meena et al. [7] have used rectangular masks to remove upper and lower eyelids. Three feature extraction methods have been proposed. They are circular and radial features, Fourier transform along radial directions and circular-mellin operator. It is reported that the circular-mellin operator gives the best result at accuracy rate of 95.45%. Y. Du et al. [8] have used grayscale invariant local texture patterns to create 1D feature. Du measure is used for template matching. This method gives over 97% accuracy for the top 5 rankings.

In our previous work,"Personal Verification and Identification via Iris Pattern Using Radon Transform" [9], we have proposed to use the concatenation of 2 preprocessed partial iris images. We enhance the image before extracting feature with Radon transform. The equal error rates (EER) are 8.3% for verification and 18% for identification.

This paper presents an improvement of our previous method mentioned above. Our previous work is briefly explained in section 2. Section 3 illustrates our improved algorithm. Template matching is discussed in section 4. Then, section 5 presents system performance evaluation and the experimental results and section 6, the conclusion.

2. OUR PREVIOUS WORK

In our previous work, "Personal Verification and Identification via Iris Pattern Using Radon Transform" [9], we have proposed a personal verification and identification system using Radon transform in order to extract iris feature. Radon transform has been utilized because the computation itself is simple and the processing time is not slow.

Our previous work consists of several parts as fol-

Manuscript received on December 16, 2006; revised on March 16, 2007.

The authors are with the Department of Computer Engineering, Faculty of Engineering Chulalongkorn University, Bangkok 10330, Thailand; E-mail: pat.ari@gmail.com, nongluk.c@chula.ac.th

lows: image preprocessing, feature extraction, template matching and the system performance test for personal identification. The first three parts are explained in the following subsections whereas the last part, in section 5.

2.1 Image preprocessing

Detection of iris boundary is the first step to be accomplished by using horizontal and vertical projection profiles [10] followed by circle detection as shown in figure 1(b). In our previous approach [9], in order to avoid eyelids and eyelashes, we have segmented and used partial iris areas on the right side, which is between -45 and 45 degrees, and on the left side between 135 and 225 degrees as shown in figure 2(a). The partial iris images are transformed from Cartesian-coordinate images into polar-coordinate images. The two images are concatenated as shown in figure 2(b) and then enhanced by global histogram equalization.

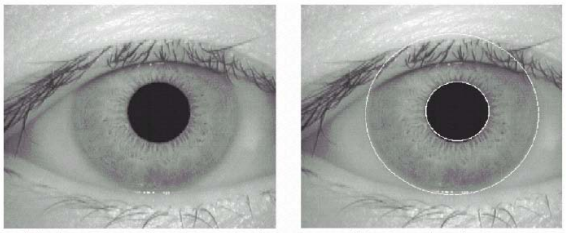

(a) An example of original image *(b) Result of iris localization of (a)*

Fig.1: *An example image from Iris boundary detection.*

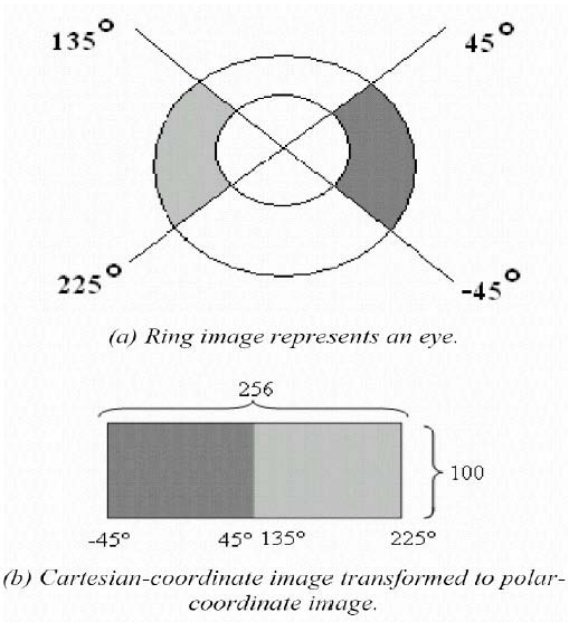

(a) Ring image represents an eye.

(b) Cartesian-coordinate image transformed to polar-coordinate image.

Fig.2: *Ring transformation from Cartesian-coordinate image to polar-coordinate image.*

2.2 Feature Extraction

Radon transform is used for feature extraction as shown in equations (1) and (2). Radon transform is a transform that is the projection of an image along specified direction [9]. The processed image is a 256x100, 8-bit grayscale image. We have selected 10 rotation steps for Radon transform. The angle starts at 0 degree and increases anti-clockwise by 18 degrees at a time. Hence, the extracted feature, which is the projection of a grayscale image, consists of 274x100 values. The number 274 refers to the most projection width of 10 rotated images. An example of Radon transform of a grayscale image is shown in figure 3. Figure 4 is an example of the extracted feature represented as a grayscale image.

$$\mathrm{R}_\theta(x') = \int_{\infty}^{-\infty} f(x'cos\theta - y'sin\theta, x'sin\theta + y'cos\theta)dy' \tag{1}$$

$$\begin{bmatrix} x' \\ y' \end{bmatrix} = \begin{bmatrix} \cos\theta & \sin\theta \\ -\sin\theta & \cos\theta \end{bmatrix} \begin{bmatrix} x \\ y \end{bmatrix} \tag{2}$$

Where f is the intensity of a pixel.

θ is the rotation angle.

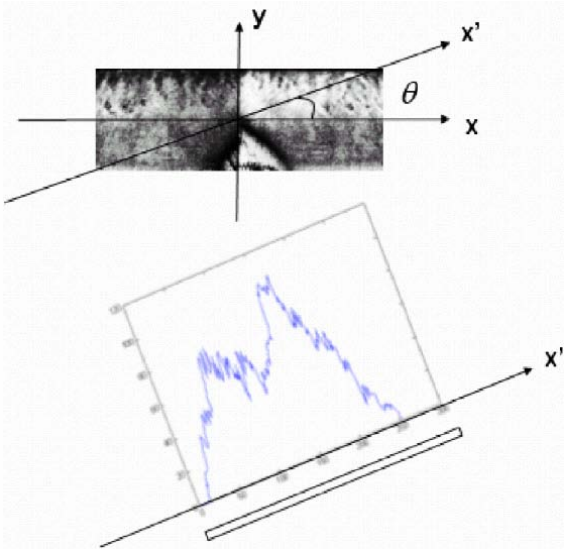

Figure.3: *Radon transform along angle θ.*

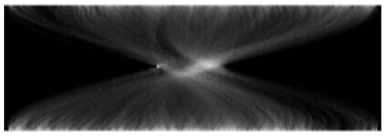

Fig.4: *An example of Radon transform that is adjusted in order to present as an image.*

2.3 Template Matching

In our previous work, we have matched templates with four distance functions which are regional correlation, Euclidean distance, absolute distance and S1 distance. From our experiments, the Euclidean distance provides the best results.

3. AN IMPROVED APPROACH

The objective of this research is to improve our previous work. Firstly, as we have noticed that the connecting area of the right and left partial iris images can cause much error for Radon transform, we change the partial iris image representation before extracting the feature via Radon transform. Secondly, we aim to achieve clearer details of iris pattern before performing Radon transform. Lastly, we attempt to improve the iris feature by decreasing the feature sensitivity due to intensity variation so that error rate can be reduced.

3.1 Changes in Partial Iris Image Representation.

Since the size of pupil varies upon light change, we normalize the polar-coordinate partial iris image to a fixed size of 128x100. Examples of the right side and the left side are shown in figure 5(d) and figure 5(e) respectively.

As mentioned above, the iris image representation before feature extraction in our previous approach [9] can cause much error for Radon transform at the concatenated border. Therefore, in this work, instead of concatenating the partial iris images before extracting the feature, we now separately extract the feature from the two partial iris images and concatenate the Radon transform results afterward.

3.2 Improving the Iris Patterns

acquisition stage may vary and can significantly impact the system accuracy, we therefore normalize all polarcoordinate iris images in the database with equations (3) and (4) [11].

$$I'(x,y) = \begin{cases} \phi_d + \lambda \ ; & if\ I(x,y) > \phi \\ \phi_d - \lambda \ ; & otherwise \end{cases} \quad (3)$$

$$\lambda = \sqrt{\frac{\rho_d (I(x,y) - \phi)^2}{\rho}} \quad (4)$$

Where $I'(x,y)$is the normalized image
ϕ_d and ρ_d are mean and variance of resultimage.
ϕ and ρ are mean and variance of originalimage.
$I(x,y)$ is the intensity at position (x,y)

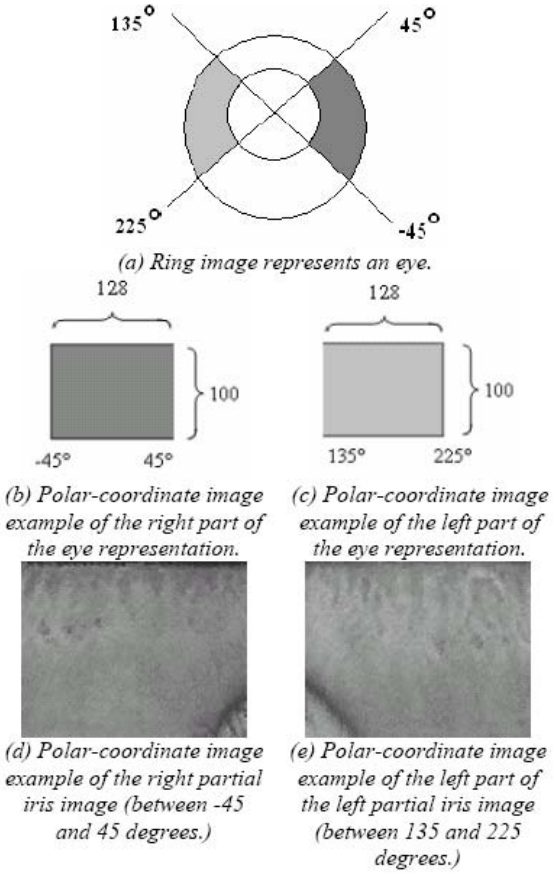

Fig.5: *Partial ring conversion to polar-coordinate of an example image..*

In this work, the mean and variance of result images are set to the average mean and average variance of all polar-coordinate partial iris images in the database.

After all iris images are normalized, they are enhanced in order to obtain clearer details of iris patterns. We have noticed that even though histogram equalization enhances iris images, it somehow lessens the details of iris patterns as shown in figures 6(a) and 6(b). Hence, in this work, we propose to apply local histogram equalization instead. It should be noted that the window size for local histogram equalization highly affects the result. For our partial iris images, the bigger the window of local histogram equalization is, the less intensity contrast and the less noises are enhanced. In this research, the window size is set at 35x35 pixels. The result image is reduced to 94x66 pixels because we ignore the sides of the image which could induce more noise from local histogram equalization. An example of the result from local histogram equalization is shown in figure 6(c).

3.3 Iris Feature Improvements

The selected feature in our previous work is the Radon transform of a grayscale image. The gray-level values can cause high variations to Radon transform

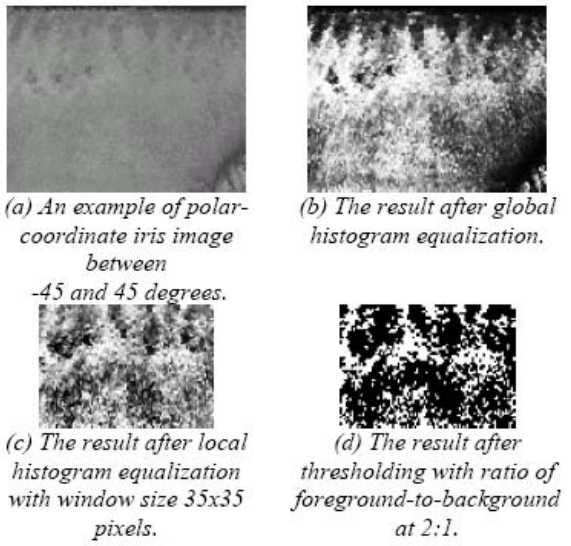

Fig.6: *The quality improvement of polar-coordinate iris image result.*

because it is the grayscale projection profile. Therefore, in attempt to lessen the Radon transform sensitivity, we use a binary image instead of a grayscale image as our input to Radon transform. In this research, the threshold is set to the value where the ratio of foreground-tobackground is 2:1. An example of the thresholded image is shown in figure 6(d).

Our feature template from Radon transform consists of the data from 10 rotation angles, from 0 degree to 180 degrees where the rotation step is 18 degrees counterclockwise. Hence, the size of the template is 115x20 values. The number 115 refers to the most projection width of the 10 rotated images and the number 20 is from ten rotation angles of the right partial iris image and ten of the left. Figure 7 is the Radon transform of the binary images representing as a gray-scale image. It is noted that the data are shown as intensities for the purpose of image representation only.

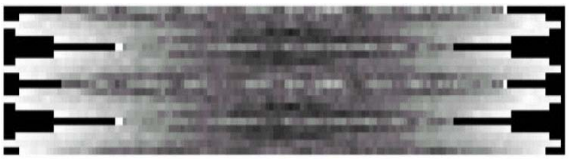

Fig.7: *An example result image of Radon transform of a binary image.*

4. TEMPLATE MATCHING

There are many template matching methods used in pattern recognition. For this research, three distance metrics are applied for personal identification test as follows.

1. Regional Correlation.

$$D_{r_\theta} = \underset{\tau}{Max}\left[\frac{\sum_{x'}\left[A_\theta(x')-\overline{A_\theta}\right]\bullet\left[B_\theta(x'-\tau)-\overline{B_\theta}\right]}{\left[\sum_{x'}\left[A_\theta(x')-\overline{A_\theta}\right]^2\right]^{1/2}\left[\sum_{x'}\left[B_\theta(x')-\overline{B_\theta}\right]^2\right]^{1/2}}\right] \quad (5)$$

2. Euclidean Distance.

$$D_e = \underset{\tau}{Min}\left[\sqrt{\sum_{x'}\left(A_\theta(x')-B_\theta(x'-\tau)\right)^2}\right] \quad (6)$$

3. Absolute Distance.

$$D_a = \underset{\tau}{Min}\left[\sum_{x'}\left|A_\theta(x')-B_\theta(x'-\tau)\right|\right] \quad (7)$$

where$_\theta(x')$ is a feature vector of iris image stored as a template in database.

$B_\theta(x')$ is a feature vector of a tested image.

$\overline{A_\theta}, \overline{B}_\theta$are the average values of feature vectors.

τ corresponds to the possible offset between the two iris templates.In our implementation,$\tau \in [-10°, 10°]$.

5. EXPERIMENTAL RESULTS

The test data and template matching methods of our improved approach are the same as those used in our previous work [9].

5.1 Testing

The iris images in our experiments are from CASIA iris database [12]. The resolution of each image is 320x280 pixels, 256 gray levels. There are totally 108 datasets from 108 users. Each dataset consists of 7 iris images.

In our experiments, we divide the data into 2 groups. The first group, consisting of 60 users, is regarded as genuine users to the system while the other group, as imposters. For genuine users, 3 images are used for registering to the system and the others are for testing the system with 3 different distance functions.

Performance of a biometric system is measured by False Acceptance Rate (FAR) and False Rejection Rate (FRR). FAR is a ratio of the number of system accepting imposters to total attempts while FRR is a ratio of the number of system rejecting the enrolled users to total attempts. Equal error rate (EER) is

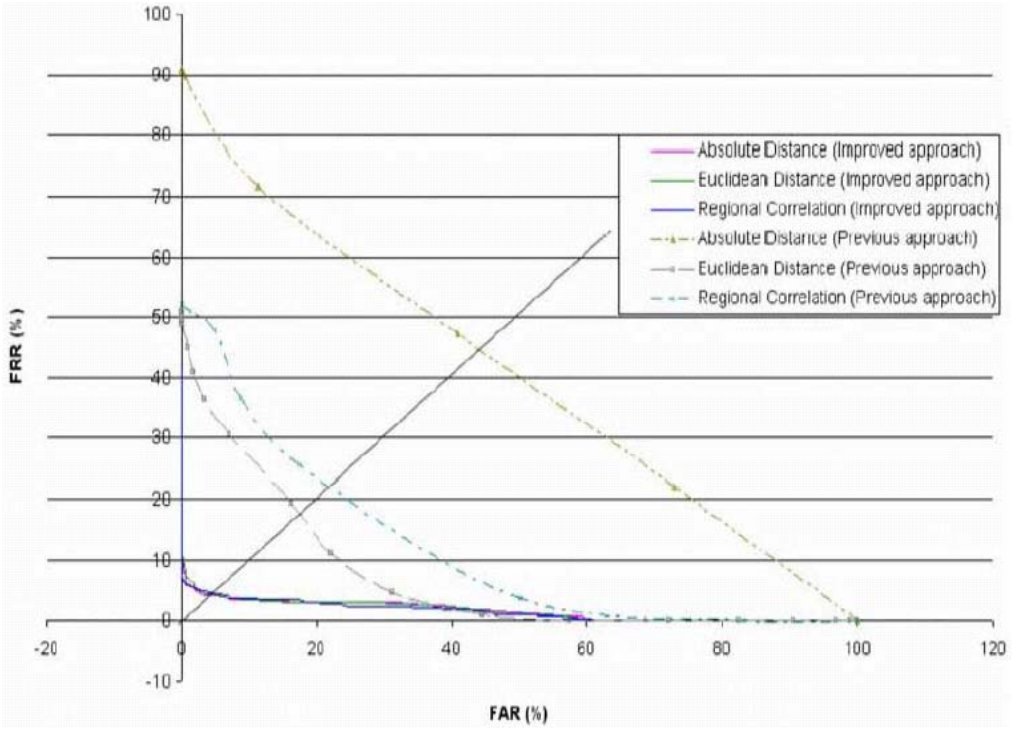

Fig.9: *ROC graph of a personal identification of our previous approach and our improved approach using 3 distance functions.*

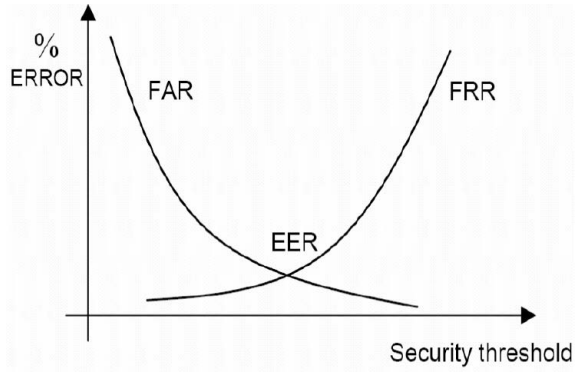

Fig.8: *A plot of FAR and FRR in varying thresholds.*

where FAR equals FRR. It is used to measure the performance in order to compare among several biometric systems. Figure 8 illustrates the FAR and FRR graph [1, 2, 3].

5.2 Experimental results

Personal identification is a process to identify a person who is registered to a system. A test data must be compared to all templates stored in the database. Therefore, it is a one-to-many matching process. The results of this step are the matching scores. The system then decides from the matching scores who the person is.

Normally, in order to calculate FAR and FRR, a score threshold must be set. If the matching score is more than threshold, the system will reject the attempting person. But if it is less than threshold, the system then identifies who the person should be. The experimental results are shown in table 1.

Table 1: *EER of personal identification systems with different distance functions.*

Distance Function	EER (%)	
	Previous Approach	Improved Approach
1. Regional Correlation	23	3.757
2. Euclidean	18	3.76
3. Absolute	44	*3.695*

From table 1, the EERs of our improved method greatly decrease for all distance functions. Absolute distance gives a little better result than Euclidean distance and regional correlation methods. It can also be clearly seen in the ROC (Receiver Operating Characteristic) graph of our personal identification systems, as illustrated in figure 9, that the system performances of the improved approach are nearly the same for all three distance functions and far better than our previous approach. Among the three distance functions, absolute distance provides the best result.

6. CONCLUSION

This research proposes an improvement of partial iris pattern identification using Radon transform. Several changes are done as follows: Partial iris representation is changed to solve the problem that errors in Radon transform arise at the connecting area of the right and left partial iris images. Local histogram equalization is applied to enhance the details of iris patterns. Lastly Radon transform is computed from a binary image rather than a grayscale image in order to reduce the feature sensitivity.

The experimental results illustrate that the performances of identification systems with our improved approach are much higher than those of our previous approach. The best EER is 3.695%, matching the features with absolute distance.

ACKNOWLEDGMENTS

The authors would like to express their appreciation to the 90th year Anniversary of Chulalongkorn University (Ratchadaphiseksomphot Endowment Fund) for the funding support, the Chinese Academy of Sciences Institute of Automation (CASIA) for the iris database, and Dr. Somying Thainimit and Dr. Vutipong Areekul for their valuable comments.

References

[1] R. P. Wildes, "Iris recognition: an emerging biometric technology," Proceedings of the IEEE, vol. 85, pp. 1348-1363, 1997.

[2] A. Jain, R. Bolle, and S. Pankanti, "Biometric: Personal Identification in Networked Society," Kluwer Academic Publishers, 2002.

[3] J.G. Daugman, "High Confidence Recognition of Persons by Rapid Video Analysis of Iris Texture," European Convention on Security and Detection, no. 408, pp. 244-251, 1995.

[4] R. Sanchez-Reillo and C. Sanchez-Avila, "Iris Recognition with Low Template Size," Third International Conference on Audio- and Video-Based Biometric Person Authentication, AVBPA 2001, vol. 2091, pp. 324, 2001.

[5] L. Ma, T. Tan, Y. Wang, and D. Zhang, " Personal identification based on iris texture analysis," IEEE Transactions on Pattern Analysis and Machine Intelligence, vol. 25, pp. 1519-1533, 2003.

[6] C. Chun and R. Chung, "Iris Recognition for Palm- Top Application," Biometric Authentication: First International Conference (ICBA04), vol. 3072, pp. 426-433, 2004.

[7] B. R. Meena, M. Vatsa, R. Singh, and P. Gupta, "Iris Based Human Verification Algorithms," Biometric Authentication: First International Conference (ICBA04), vol. 3072, pp. 458-466, 2004.

[8] Y. Du, R. Ives, D. Etter, T. Welch and C-I. Chang, "A One dimensional approach for iris identification," Proceedings of SPIE, Biometric Technology for Human Identification, vol.5404, pp.237-247, 2004.

[9] P. Ariyapreechakul and N. Covavisaruch, "Personal Verification and Identification via Iris Pattern Using Radon Transform," Proceedings of the first National Conference on Computing and Information Technology, Nontaburi, pp. 287-292, 2005.

[10] R. C. Gonzalez, and R.E. Woods, Digital Image Processing, U.S.A.: Prentice-Hall, Inc., 2002.

[11] L. Hong, Y. Wan, and A.K. Jain, "Fingerprint Image Enhancement: Algorithm and Performance Evaluation," IEEE Transaction Pattern Analysis and Machine Intelligence, Vol.20, pp.777-789, 1998.

[12] Chinese Academy of Sciences Institute of Automation, "Database of 756 Grayscale Eye Image," http://www.sinobiometrics.com, version 1.0, 2003.

Pattraporn Ariyapreechakul received a B.Eng degree in Computer Engineering from King Mongkuts Institute of Technology Ladkrabang, Thailand, in 2003. She is now a graduate student in M.Eng. Program in Computer Engineering at Chulalongkorn University, Thailand. Her research interests include biometrics and image processing.

Nongluk Covavisaruch received an M.S.degree in Electrical Engineering from University of Missouri-Columbia and an M.A. (Language and International Trade) from Eastern Michigan University. She is an Assistant Professor of the Department of Computer Engineering at Chulalongkorn University. She has joined the department since 1990 and teaches both undergraduate and graduate courses in digital image processing. She served as the head of Computer Graphics and Computer Imaging Laboratory from 2001- 2005. Her research interests include image and vision computing techniques, biometrics, biomedical image processing, image processing and computer vision applications and colors in computers.